

Development and Evaluation of a novel Robotic Platform for Gait Rehabilitation in Patients with Cerebral Palsy: CPWalker

C. Bayón¹, O. Ramírez¹, J.I. Serrano¹, M.D. Del Castillo¹, A. Pérez-Somarriba³, J.M. Belda-Lois², I. Martínez-Caballero³, S. Lerma-Lara³, C. Cifuentes⁴, A. Frizera⁵ and E. Rocon^{1,5}

1. Neural and Cognitive Engineering group, Centro de Automática y Robótica, Consejo Superior de Investigaciones Científicas, 28500 Arganda del Rey, Madrid, Spain.
2. Instituto de Biomecánica de Valencia, Valencia, Spain.
3. Hospital Infantil Universitario Niño Jesús, Madrid, Spain.
4. Colombian School of Engineering Julio Garavito, Bogota, Colombia.
5. Graduate Program on Electrical Engineering, Universidade Federal do Espírito Santo, Vitória-ES, Brazil.

Correspondence to: Cristina Bayón, Neural and Cognitive Engineering group, Centro de Automática y Robótica, Consejo Superior de Investigaciones Científicas,

Ctra Campo Real km 0.2 - La Poveda-Arganda del Rey

28500 Madrid SPAIN

E-mail: cristina.bayon@csic.es

ABSTRACT

The term Cerebral Palsy (CP) is a set of neurological disorders that appear in infancy or early childhood and permanently affect body movement and muscle coordination. The prevalence of CP is two-three per 1000 births. Emerging rehabilitation therapies through new strategies are needed to diminish the assistance required for these patients, promoting their functional capability. This paper presents a new robotic platform called CPWalker for gait rehabilitation in patients with CP, which allows them to start experiencing autonomous locomotion through novel robot-based therapies. The platform (smart walker + exoskeleton) is controlled by a multimodal interface that gives high versatility. The therapeutic approach, as well as the details of the interactions may be defined through this interface. CPWalker concept aims to promote the earlier incorporation of patients with CP to the rehabilitation treatment and increases the level of intensity and frequency of the exercises. This will enable the maintenance of therapeutic methods on a daily basis, with the intention of leading to significant improvements in the treatment outcomes.

HIGHLIGHTS:

- Rehabilitation with free displacement and not restricted to a treadmill.
- Integration of central nervous system into therapies.
- Postural control and partial body weight support for individuals with more severe disorders.
- "Assist as needed" approach.
- Locomotion strategy based on laser sensor.

KEYWORDS: Cerebral Palsy, Rehabilitation Robotics, Gait, Posture, Exoskeleton.

1 **1. Introduction**

2 Cerebral Palsy (CP) could be defined as a disorder that appears in infancy and
3 permanently affect posture and body movement but does not worsen over time [1]. CP
4 is often associated with sensory deficits, cognitive impairments, communication and
5 motor disabilities, behavior issues, seizure disorder, pain and secondary musculoskeletal
6 problems [1]. CP affects between two to three per 1000 live-births, reported to the
7 European registers by the Surveillance of Cerebral Palsy European Network (SCPE)
8 [2], and there is a prevalence of three to four per 1000 among school-age children in
9 USA [3].

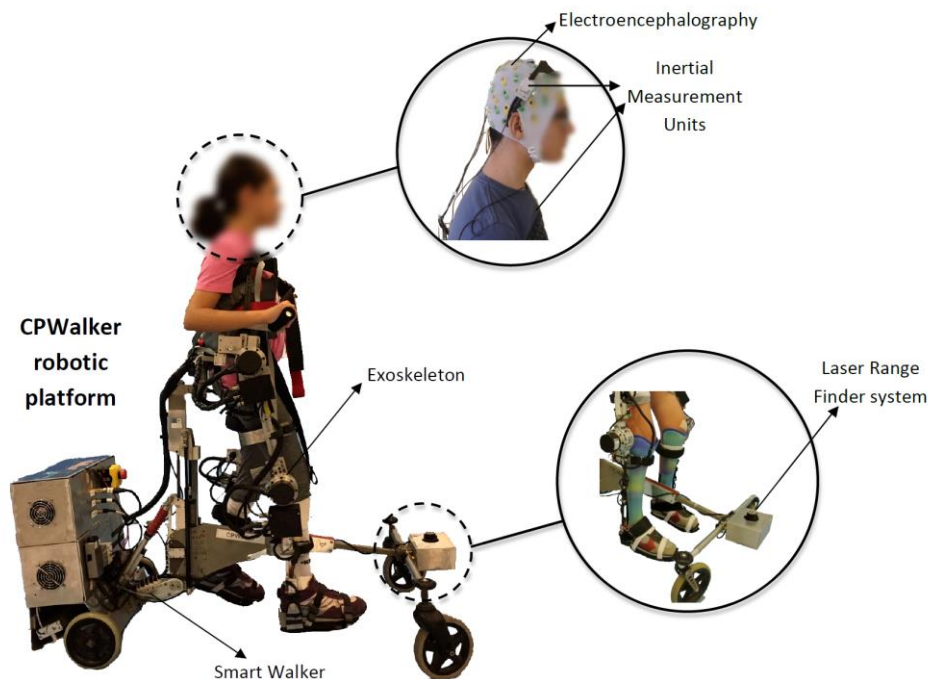
10 In some cases, the development of a secondary musculoskeletal pathology contributes
11 to loss of function, gait impairments, fatigue, activity limitations, and participation
12 restriction. Several technological advancements have been introduced into the field of
13 rehabilitation to complement conventional therapeutic interventions. Intense task-
14 related strategies, comprehensive combination of non-invasive treatment, surgical
15 interventions and new technologies have been initiated to improve rehabilitation
16 strategies [4]. These novel technologies, such as robot-assisted gait training or other
17 computer-assisted systems have been primarily developed for adults [5]. Nevertheless,
18 after technological adaptations, these therapies have been implemented in the pediatric
19 field [6]. Preliminary results have supported the feasibility of these novel approaches in
20 the clinical context [7], [8]. More specifically, robot-based therapy is a safe treatment
21 option with no severe side effects [9]. In addition, clinical experience suggests that gait
22 training in children with considerable cognitive deficits could be conducted even more
23 effectively using robot-assisted therapy rather than conventional training [6].

24 Traditionally, robotic strategies have been focused on the Peripheral Nervous System
25 (PNS) supporting patients to perform repetitive movements (a “Bottom-Up approach”).
26 However, CP primarily affects brain structures, and thus suggests that both PNS and
27 Central Nervous System (CNS) should be integrated into a physical and cognitive
28 rehabilitation therapy [10]. Current studies manifest that such integration of the CNS
29 into the human-robot loop maximizes the therapeutic effects, especially in children.
30 This approach is known as "Top-Down" approach [10]: motor patterns of the limbs are
31 represented in the cortex, transmitted to the limbs and feedback to the cortex. Although
32 this approach has been previously studied in other populations (e.g. stroke [11], Spinal
33 Cord Injury [12]), there is a lack of studies in Cerebral Palsy [13].

34 On the other hand, rehabilitation with progressive reduction of partial body weight
35 support (PBWS) coinciding with over-ground walking encourages the patients and it is
36 a motivated condition for recovery in childhood [14].

37 In this paper we propose a new robotic platform (CPWalker, Figure 1) with the aim of
38 supporting novel therapies following a "Top-Down" approach for CP rehabilitation. The
39 platform is composed by a smart walker with PBWS and autonomous locomotion for
40 free over-ground training, and a wearable robotic exoskeleton for joint motion support.
41 The interaction between the patients and the robotic device will take place through a
42 Multimodal Human-Robot Interface (MHRI) consisting in a set of sensors attached to
43 the device, allowing the users to control the system through different modalities that are
44 commented in the next points. We focus our attention on children with CP, who present
45 increased brain plasticity compared to adults, and are more likely to have a change in
46 motor patterns following an intervention [15]. With this platform we want to contribute
47 beyond reducing the clinician's effort or increasing the duration of the treatment, giving
48 the novelties of: i) free movement (not restricted to treadmill training) to enhance the

49 subject's motivation; ii) tailored therapies depending on the user's needs through Assist
 50 as Needed (AAN) strategies to increase the patient's participation; iii) the use of
 51 different sensors to improve the rehabilitation, controlling posture during robot-based
 52 therapy; iv) integration of CNS to intensify the effects of the therapy.



53

54 **Figure 1. CPWalker platform (smart walker and exoskeleton) and the technology used in the multimodal**
 55 **human-robot interface (MHRI): electroencephalography unit, inertial sensors for postural control and laser**
 56 **range finder.**

57 This paper presents the development of such a platform, which is called CPWalker.
 58 Next section introduces the aspects related to the conceptual design of the platform and
 59 the description of the different components of CPWalker. In section 3, the multimodal
 60 interface to enable the implementations of "Top-Down" rehabilitation strategies is
 61 presented. The elemental control strategies proposed for CPWalker are given in section
 62 4. Section 5 discusses the control architecture and the communication between its
 63 components. Preliminary technical validations are introduced in section 6. Finally,
 64 section 7 reported the discussions and conclusions of the work.

65 2. Robotic platform

66 CPWalker is a robotic platform to help patients with CP (primarily children) to recover
 67 the gait function through rehabilitation training. The definition of the conceptual design
 68 of the platform was undertaken based on the results of several interviews with a
 69 population composed by 4 children with CP, 10 relatives, 4 doctors and 5
 70 physiotherapists. The evaluation of these results provided some requirements, features
 71 and functionalities that were needed and should be integrated in the novel device. We
 72 defined the neurophysiological aspects for the development of each subsystem:
 73 anatomical joint and muscle groups target by our platform, as well as the kinematic and
 74 kinetic profile patterns of pathological gait of subjects with PC. The result of this
 75 analysis (Table I) enabled the consortium to: i) identify the needs and demands of gait
 76 rehabilitation for different user's profiles; ii) recognize the problems and benefits
 77 presented by the current walkers; iii) identify current gaps in the market; iv) determine
 78 the features and functionality needed in the new walker; and v) determine the
 79 requirements of accessibility and usability to be considered in the design and
 80 development.

81 **Table I. Results of the interviews that serve as base for the conceptual design of CPWalker**

Criteria for the Conceptual Design of CPWalker		
To correct problems which concern about	To apply usability criteria which allow	To improve the rehabilitation through
<ul style="list-style-type: none"> – Changing the previous gait pattern – Removing the crouch gait – Dissociating each side of the body – Improving the force in muscles 	<ul style="list-style-type: none"> – To improve the balance – Patient's PBWS – To enhance the force 	<ul style="list-style-type: none"> – Reducing the caregiver's physical effort – Allowing over-ground displacement in real rehabilitation environments – Including CNS into the therapies

82

83 Based on this information we defined the conceptual design and the main requirements
84 of CPWalker platform. As a result, we decided to build our robotic platform based on
85 the commercially available device, NFWalker (Made For Movement, Norway). Some
86 mechanical modifications on the NFWalker were carried out in order to transform this
87 passive device into an active rehabilitation platform. The proposal of CPWalker
88 platform is similar to others adopted before [7], [14], but in this case we intend to
89 design a fully active rehabilitation robotic platform, which will enable us to implement
90 robot-based therapies according to the "Top-Down" approach. As a result, CPWalker
91 will allow more intense exercises than passive devices. In order to do so, we
92 incorporated four active systems in both the walker and the exoskeleton: i) a drive
93 system of the platform; ii) a PBWS system; iii) an active system for the adaptation of
94 hip height; and iv) a system for controlling joint motion of the exoskeleton. These
95 systems will be described in depth in the following subsections.

96 **2.1. Smart walker**

97 The smart walker of CPWalker was designed with the aim of giving the necessary
98 support and balance in gait rehabilitation of children with CP. The structure may resist a
99 total maximum weight of 80kg (exoskeleton + patient). The systems included in the
100 smart walker are:

101 **2.1.1. Drive system**

102 This system is located in the back wheels, and it provides the translation movement
103 required to achieve the necessary support for an ambulation over-ground treatment in
104 real rehabilitation environments, instead of treadmill training (Figure 2). It is composed
105 by the following subsystems:

- Actuators: The traction system is constituted by two gearmotors K80 63.105 (Kelvin, Spain) coupled to each rear wheel. Motors work individually, providing independent speed to left and right wheels. The speed range of the device is encompassed between $[-0.60, +0.60]$ m/s.
- Sensors: We installed two encoders, one at each traction engine. Information provided by the encoders is used to control the velocity of the translation.

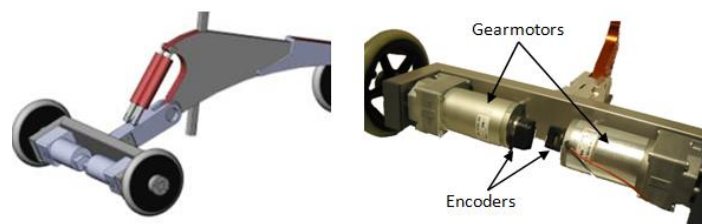


Figure 2. Drive system of CPWalker

2.1.2. Partial body weight support system

This system (Figure 3) is responsible for the control of the discharge of user's body weight. The ability of discharging a partial user's weight during gait improves the patients' rehabilitation because they have to use less activity to neutralize the gravity, and can take advantage of their residual force to learn and coordinate movements [16]. It aims at making easier the exercises along the first sessions (when the patient is weaker) or with users with a greater Gross Motor Function Classification System (GMFCS) score [17]. The effectiveness of the PBWS in robotic rehabilitation has been demonstrated previously [14], [18], [19]. The actuators and sensors of this system are:

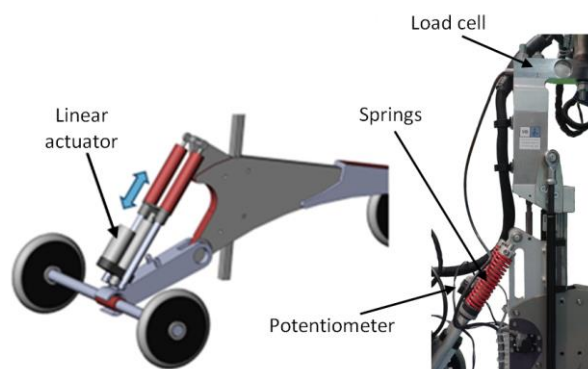
- Actuators: this system consists of an electric linear actuator CAHB-10-B5A-050192-AAAP0A-000 (SKF, Sweden), which with an input voltage of 24Vcc can achieve 1000N of load. This actuator compresses and decompresses the original springs of NFWalker (Figure 3 left), and the user's weight is controlled

127 by this compression and decompression. It allows a significant unloading
 128 respect to the ground up to 45kg.

129 • Sensors: The sensory part of the PBWS system is composed by a potentiometer
 130 and a load cell:

131 ○ Potentiometers: the elevation system is equipped with one potentiometer,
 132 which measures the compression or decompression of the springs of the
 133 suspension system, and it is located between them (Figure 3 right). This
 134 measure is used to implement the fine control of the user's weight
 135 discharge.

136 ○ Load cell: this force sensor is integrated into the walker structure (Figure
 137 3 right) in order to measure the amount of user's weight that is supported
 138 by the robotic platform. This information is therefore used for the control
 139 system.



140

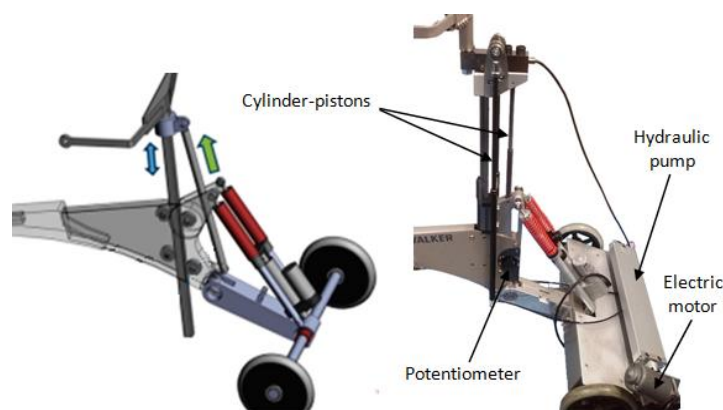
141 **Figure 3. System for PBWS of the patient**

142 2.1.3. System for the adaptation of hip height

143 This system is used to adapt the robotic platform to different anthropometric measures
 144 by adjusting the hip joint of the exoskeleton at a specific distance from the ground
 145 (Figure 4). The system is able to elevate the patients from the floor and position them

146 with legs stretched. Therefore, the user can walk without restrictions. In order to
 147 implement such actions, it is composed by the following actuators and sensors:

- 148 • Actuators: this system is activated by a linear actuator E21BX300-U-001
 149 (Bansbach easylift, Germany) composed by a hydraulic pump and two cylinder-
 150 pistons. The hydraulic pump is controlled by an electric motor. The pistons are
 151 connected to the hip joint of the robot and by controlling its displacement the
 152 system may control the height of the user's hip in relation to the ground (Figure
 153 4). With a stroke length of 300 mm, this actuator is able to generate forces high
 154 enough to elevate the child. The cylinders work in parallel through a slideway
 155 that supports the bending moments generated by the user's weight.
- 156 • Sensors: this system has one potentiometer for the height regulation system,
 157 which is located in the docking between the exoskeleton and walker (Figure 4).
 158 The potentiometer changes the measure according to the hip elevation with
 159 respect to the walker platform. This parameter gives information about the
 160 position of the hydraulic linear actuator.



161

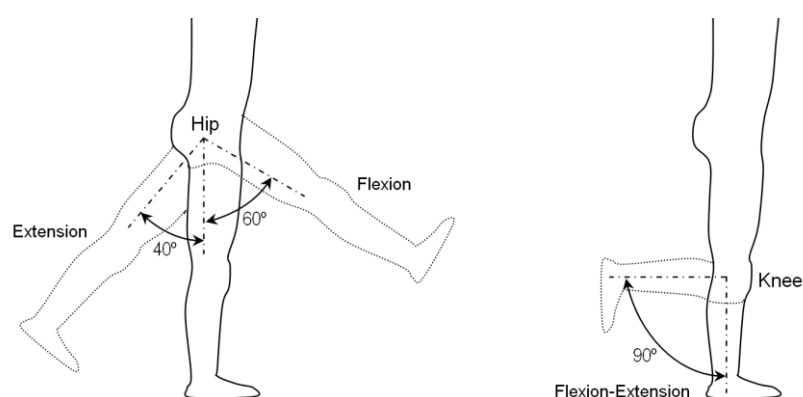
162

Figure 4. System for the anthropometric adaptation of hip

163

2.2. Exoskeleton

164 The exoskeleton of CPWalker has a kinematic configuration similar to the human body,
 165 and it can implement guided and repetitive movements to the user's lower limbs in the
 166 sagittal plane. The structure of the exoskeleton is based on the original NFWalker
 167 device, in which the requirements of actuators have been added, based on previous work
 168 [20]. Aluminum 7075 is mainly used in the structure of the exoskeleton and joints, due
 169 to its mechanical resistance and lightweight. The whole design of the exoskeleton is
 170 lightweight and, at the same time, rigid and strong in order to allow walking and
 171 increase strength and endurance of people with mobility disorders, in particular children
 172 with CP. In order to make the robot compatible with different users, the length of the
 173 structure can be adjusted to different patient's anthropometric measures. In addition, the
 174 exoskeleton prevents displacements of lower limbs to abnormal positions. The device
 175 has been designed for over-ground walking training, and according to this, the
 176 maximum allowed range during walking is: 60° for hip flexion, 40° for hip extension,
 177 90° for knee flexion and 0° for knee extension (Figure 5). The movable range ensures
 178 the necessary motion for proper gait rehabilitation. For safety reasons, the range
 179 limitation is kept by both hardware (adjustable end-stops) and software.

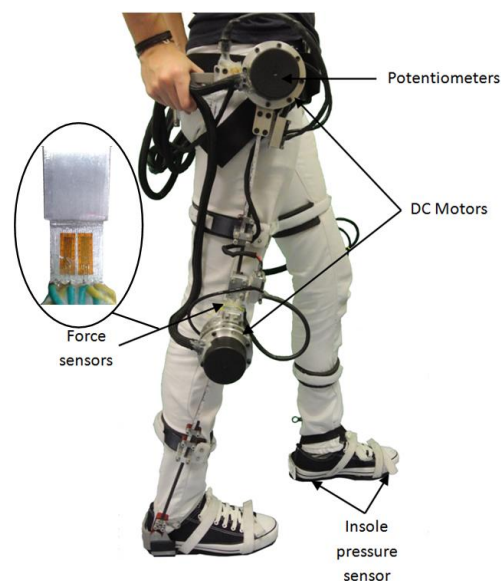


180
 181 **Figure 5. Range of motion of the different joints of the CPWalker exoskeleton**

182 2.2.1. System for the control of joints movements

183 The exoskeleton system is composed by six active joints (both hips, knees and ankles),
 184 although at present it only has actuated hips and knees, while the ankle is left free to
 185 move (Figure 6).

- 186 • Actuators: the actuation of each exoskeleton joint is composed by a harmonic
 187 drive coupled with a brushless flat DC motor EC-60 flat 408057 (Maxon ag,
 188 Switzerland). The harmonic drive mechanism CSD-20-160-2AGR (Harmonic
 189 Drive LLC, USA) was selected due to its capacity of working with high gear
 190 reduction ratios, allowing ensemble position accuracy with a low
 191 weight/volume ratio. The gear transmission of the joint is 1:160. This setup was
 192 adopted since it allowed the design of a compact actuation system [21]. The
 193 assembly (Figure 7) provides an average torque of 35 Nm, which is in
 194 accordance with the requirements of [22], [23].

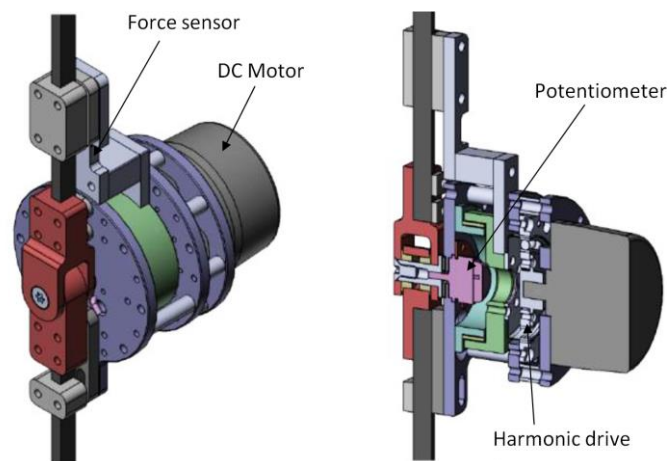


195

196 **Figure 6. User wearing the exoskeleton of CPWalker**

- 197 • Sensors: The sensors included in this system are:
 - 198 ○ Potentiometers: The exoskeleton has one potentiometer placed
 - 199 concentrically to each joint assembly (Figure 7). Voltages values

- 200 received from these potentiometers are converted to angle values, which
 201 provide information on the angular position of each joint. This
 202 information is used for the implementation of the position and
 203 impedance controls.
- 204 ○ Force sensors: we have included force sensors, based on strain gauges,
 205 in the metal rods of the exoskeleton, which are coupled with the joints.
 206 These sensors are responsible for the measurement of the interaction
 207 forces between the robot and human body. Strain gauges are connected
 208 in a complete Wheatstone bridge circuit with the purpose of achieving
 209 higher sensitivity [21].
 - 210 ○ Insole pressure sensor: CPWalker uses two force-sensing resistors (FSR)
 211 for each insole (one for the heel and another for the toe). These sensors
 212 provide information related to the footsteps of the user, useful to assess
 213 the gait pattern of the patient.



214

215

Figure 7. Schematic drawing of joint assembly of CPWalker

216 3. Multimodal Human-Robot Interface (MHRI)

217 A MHRI is an interface designed with the aim of integrating both the information of
218 CNS and PNS in order to create a communication bus between the human subject and
219 the robotic device. The rationale of the MHRI of CPWalker is to take into account the
220 patient's intention to promote physical and cognitive interventions, and in a second
221 place, to provide a high versatility to the platform allowing greater adaptability of the
222 therapies to the patient's needs.

223 Several technologies are used to address these objectives, but in this case, the
224 interaction between the child and the robotic platform will take place through a MHRI
225 consisting of: i) an electroencephalographic (EEG) acquisition unit, used as a method to
226 take into account the patient's intention; ii) inertial measurement units (IMUs) to
227 improve the patient's postural control; and iii) a Laser Range Finder (LRF) to measure
228 the human locomotor patterns and to control the robotic platform accordingly. The
229 rationale of this multimodal interface is to allow integrated PNS and CNS into physical
230 and cognitive interventions. MHRI interaction with therapeutically selected tasks will
231 promote the re-organization of motor planning brain structures and thus, integrating
232 CNS into the therapy [10].

233 **3.1. EEG acquisition unit**

234 Promoting the participation of CNS in the rehabilitation strategy implies knowing and
235 modulating the role of patients' brain activity depending of their motor capability. A
236 non-invasive way for achieving this is to capture the electrophysiological activity
237 related to motor behavior by EEG sensors placed along the patients' scalp. Based on
238 such signals, the aim is to build a brain computer interface for initiating the
239 rehabilitation therapy. Additionally, this system will enable to assess the changes
240 induced on the brain by the implemented robot-based therapies.

241 The EEG control in CPWalker (Figure 1) is proposed as a method to begin the therapies
242 according to the patient's intention. The process carried out to integrate the EEG into the
243 MHRI comprises two stages: i) a first early phase aimed at remodeling cortical activity
244 related with gait; ii) a second phase where the subject controls actively the beginning of
245 the robot-based therapy on the CPWalker platform. In the first phase of training with
246 EEG, the child is lain on a bed and uses a pair of virtual reality glasses Oculus Rift
247 (Oculus, United States) through he/she can see a virtual environment in first person.
248 Once the subjects have trained with the virtual reality glasses and they dominate the
249 control of the EEG signals, they are prepared to implement this strategy into the robotic
250 platform.

251 **3.2. IMUs sensors**

252 IMUs sensors (TechMCS, Technaid, Spain) are used in CPWalker (Figure 1) to give
253 feedback to the patients when they lose the control of the desirable orientation of the
254 body. The system measures the orientation of the child's trunk and head. This
255 information was a request of our clinical partners since it is a parameter of paramount
256 importance due to with IMUs-based interface we can report to therapists about therapy
257 progress and motor evolution of children with CP [24]–[26]. These exercises with IMUs
258 consist in giving acoustic feedback to the users when subject's trunk or head are not in a
259 proper position. The aim is to correct the patient's crouch gait and to achieve a better
260 extended hip position.

261 **3.3. Laser Range Finder**

262 The subsystem to detect the user's legs location in CPWalker is composed by a LRF
263 sensor URG-04LX (Hokuyo, Japan) that is able to scan 240° and the legs detection
264 module (Figure 1). The main controller receives a full sample of the LRF scanning, and

265 an algorithm calculates the position of the legs in real time. The sensor is installed on
266 the front of CPWalker at a height of 15 cm from the floor, in order to assess legs
267 movements.

268 The leg detection approach presented in this work combines techniques presented in
269 [27], [28], and it is split into four basic tasks: i) LRF data pre-processing; ii) transitions
270 detections; and iii) extraction of pattern and estimation of legs coordinates. In the pre-
271 processing phase, the delimitations of the right leg zone and left leg zone are performed.
272 Inside of these zones the transitions associated with each leg are identified to define the
273 leg pattern. After that, the distances are calculated in relation to the middle point of each
274 leg. The legs detection module returns the distances of the left and right legs, d_l and d_r
275 respectively. This interface will enable clinicians to access a vast amount of information
276 related to the progress of the therapy, which will reveal a deeper understanding of the
277 underlying mechanisms relating to the development of the therapy. Based on this
278 approach, we plan to develop a subject-specific framework where robot assessment will
279 inform robot therapy.

280

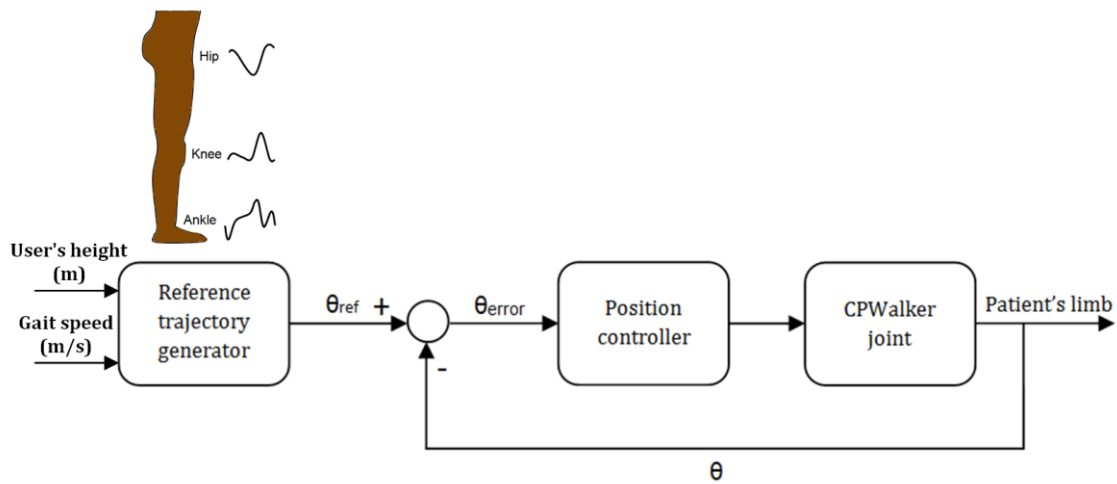
281 In a nutshell, CPWalker MHRI constitutes a novel means to integrate the CNS and PNS
282 into the robotic therapy. First, online characterization of the level of attention (at the
283 CNS) and of the neural drive to muscle (at the PNS) will permit to optimize the therapy,
284 in terms of intensity and duration, for each user. Secondly, it enables the investigation
285 of the motor patterns (at the CNS and PNS) as a means to objectively assess the
286 outcome of the therapy, and also elucidate the neural mechanisms that mediate such
287 recovery.

288 **4. CPWalker basic functions**

289 This section describes the different lower-level controllers developed for the control of
290 basic functions of the robotic platform. These basic control strategies, in combination
291 with information provided by the multimodal interface and the different sensors
292 distributed along the platform, will support the implementation of various novel
293 therapies, which will be in accordance with the opinion of our clinical partners. Gait
294 training will be provided according to the level of disability while encouraging patient's
295 participation in the training process. CPWalker robot may use trajectory or impedance
296 control as the base of training therapies that will be developed in the future. These
297 strategies may be combined, selecting different subtasks of walking for each controller.
298 We expect that this possibility will improve the common rehabilitation, insomuch as the
299 therapy is more adapted to the subject's necessities. Moreover, we include a locomotion
300 strategy based on LRF sensor as novel concept of basic strategy. The LRF sensor will
301 work when zero-force control is selected in the exoskeleton. In this case, will be the
302 patient who controls the velocity of the translation through the movement of the lower
303 limbs.

304 **4.1. Trajectory control strategy**

305 Trajectory tracking or position control is a strategy based on the principle of guiding the
306 joints of the user's lower limbs following fixed reference gait trajectories, [29]–[31]. It
307 consists on an internal control loop that uses the error (θ_{error}) provided by the difference
308 between a reference of normal gait pattern (θ_{ref}) and the angle measured by the
309 potentiometers on each exoskeleton joint (θ), (Figure 8).



310

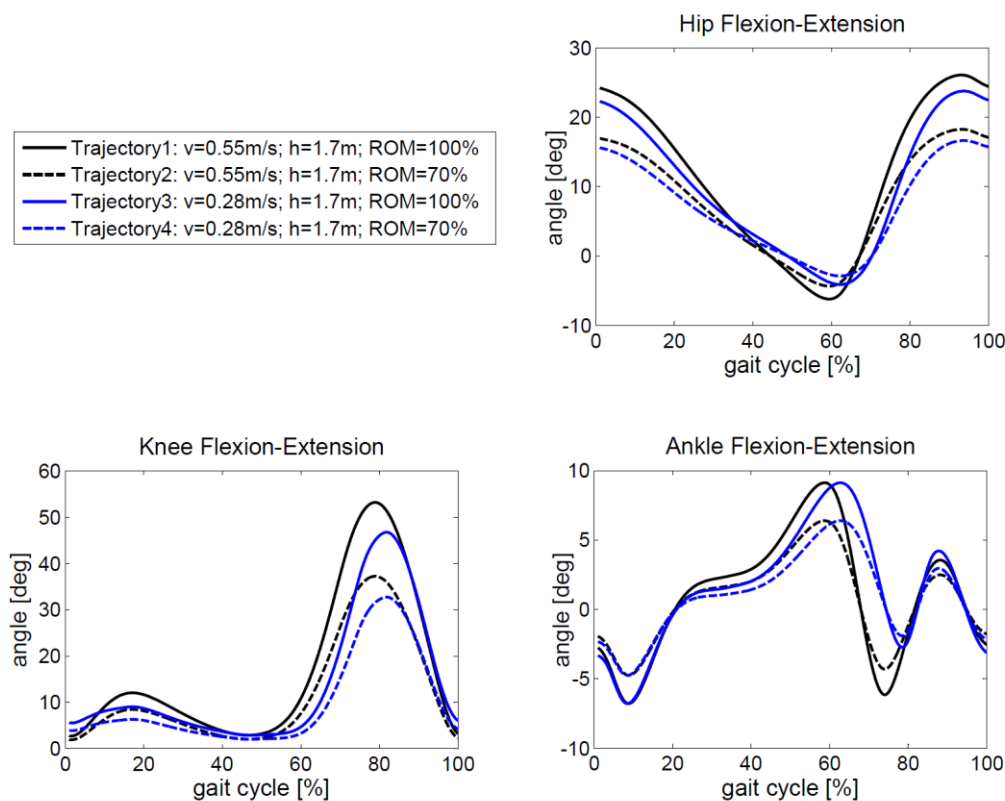
311 **Figure 8. Trajectory control algorithm of each joint of the exoskeleton. The error of each joint (θ_{error}) passes**
 312 **through the *Position Controller* box, which is a proportional controller whose parameters are individually**
 313 **selected for each joint of the exoskeleton.**

314 An important question for gait rehabilitation robots is how to assist the patient with the
 315 minimum interaction forces between robot and human. This implies that subjects will
 316 be able to walk more naturally maintaining the safety, stability and effectiveness of the
 317 system. In order to achieve this, the gait pattern applied by the robotic device must be
 318 adapted both to the individual user and to the characteristics of the gait. The reference
 319 trajectories of CPWalker platform are generated according to the algorithm presented by
 320 Koopman et al. in [32], which reconstructs reference joints trajectories based on user's
 321 height and gait speed. These reference trajectories consist of normal gait patterns
 322 represented by joint angles (θ_{ref}). The controller of each joint is responsible of ensuring
 323 the guidance of its own motion in order to get a correct normal gait pattern in the whole
 324 exoskeleton. As a result, the generated trajectory for CPWalker corresponds with a
 325 matrix of three columns (hip, knee and ankle), while the rows are the angles along the
 326 gait cycle (Equation 1).

$$\theta_{error} = \theta_{ref} - \theta = \begin{pmatrix} \theta_{refHip} \\ \theta_{refKnee} \\ \theta_{refAnkle} \end{pmatrix}^T - \begin{pmatrix} \theta_{Hip} \\ \theta_{Knee} \\ \theta_{Ankle} \end{pmatrix}^T = \begin{pmatrix} \theta_{errorHip} \\ \theta_{errorKnee} \\ \theta_{errorAnkle} \end{pmatrix}^T \quad (1)$$

327

328 With this simple strategy, the exoskeleton will be able to guide patient's lower limbs
 329 following reconstructed normal reference trajectories for any given speed or percentage
 330 of range of motion (ROM). An example of that is given in Figure 9.



331

332 **Figure 9.** Changes in reference trajectories for hip, knee and ankle flexion-extension depending on the
 333 different parameters as percentage of ROM applied and gait speed.

334 4.2. Impedance control strategy

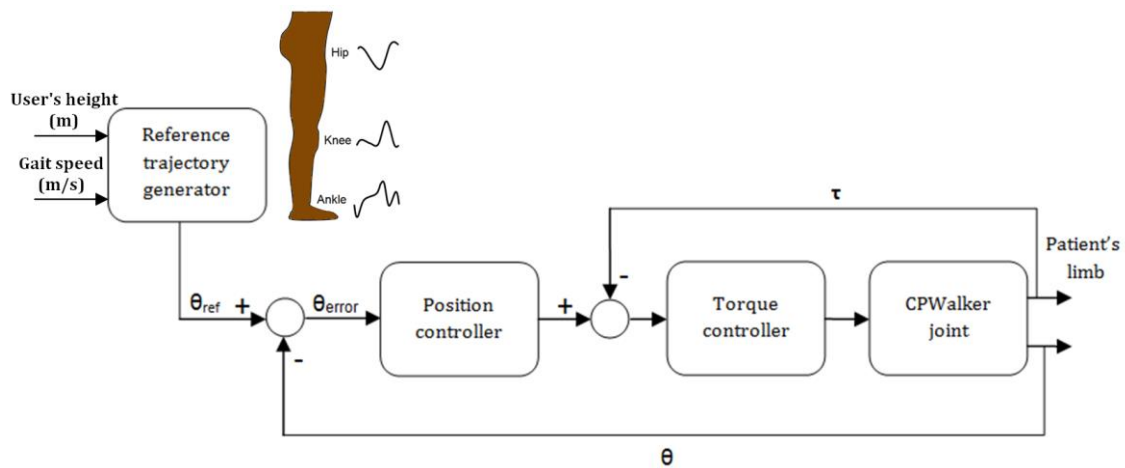
335 Although position control has been proven with positive results in several cases [33],
 336 [34], robot-based therapies might be optimized in order to increase the patient's
 337 participation. The impedance of a system ($Z(s)$) is defined as the relation between the
 338 force of this system ($F(s)$) against an external movement imposed upon it and the
 339 movement itself ($\theta(s)$), (Equation 2 and 3). The concept was introduced by Hogan in
 340 1985, [35].

$$Z(s) = \frac{F(s)}{\theta(s)} = I \cdot s^2 + B \cdot s + k \quad (2)$$

$$f = I \cdot \ddot{\theta} + B \cdot \dot{\theta} + k \cdot \theta \quad (3)$$

341 In Equations 2 and 3: f is force, I inertia, B damping and k stiffness of the system. θ , $\dot{\theta}$
 342 and $\ddot{\theta}$ are position, velocity and acceleration of the robot respectively.

343 Following the impedance concept developed by Jezernik [31], and Riener et al. [36], for
 344 the Lokomat robotic trainee, we implemented an algorithm that attempts to prevent
 345 undesired efforts on patients' lower limbs and, most important, to apply the philosophy
 346 of AAN to take advantage of patients' residual movement. The method considers the
 347 human-exoskeleton interaction to allow a variable deviation from the predefined
 348 reference trajectory, [29]–[31], [36]. The approach proposed (Figure 10) is based on a
 349 cascaded *position and force controllers*, whose internal loop is able to track force
 350 profiles in a determined bandwidth. In order to perform the parameters identification for
 351 both *position and torque controllers*, we took into account that CPWalker moves with
 352 sufficiently low values of velocity and acceleration and, consequently, the effects of
 353 inertia and damping could be disregarded. Besides, the adjustment followed empiric
 354 trial and error calibrations without human users. The *torque controller* was adapted in
 355 first place, keeping the proportional *position controller* equals to zero. Once we ensured
 356 a proper torque tracking with a zero set point, we started to adjust the external position
 357 loop, which tries to perform the generated trajectories in joint-space, if the force
 358 detected by the strain gauges of the exoskeleton is close to zero. The relation between
 359 both loops determines the impedance applied by the exoskeleton to user's lower limb
 360 movements.

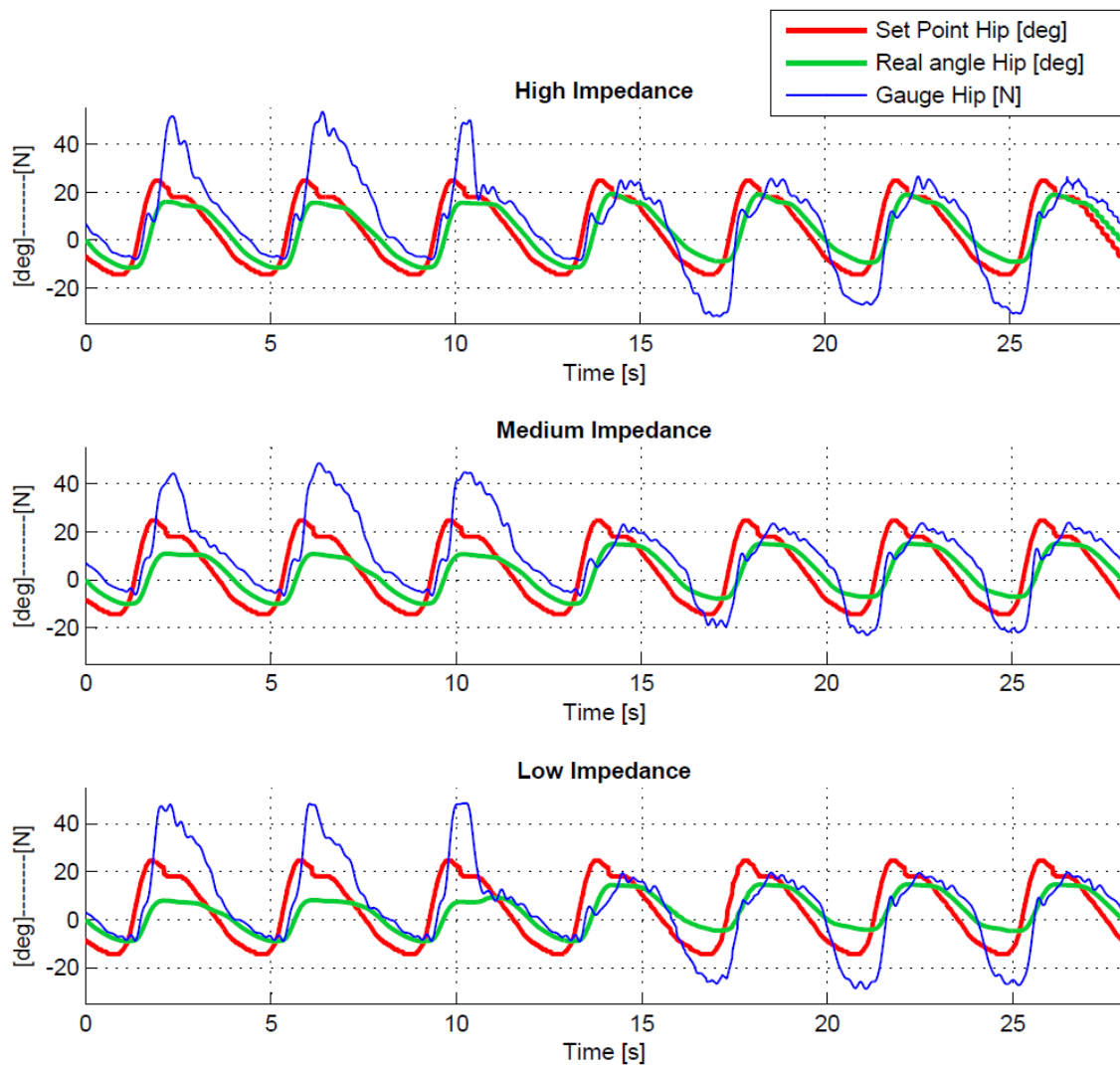


361

362

Figure 10. Impedance control algorithm of each joint of the exoskeleton.

363 Following this approach, the impedance control algorithm of CPWalker was set to
 364 provide three levels of AAN: i) high impedance (more proximal to a pure trajectory
 365 tracking); ii) medium impedance; and iii) low impedance (more proximal to patient in
 366 charge mode). The relations between the extremes of impedance modes (high and low
 367 modes) respect to the medium impedance were determined increasing and decreasing
 368 around 50% the impedance parameters. Consequently, if the position controller is
 369 higher, the torque controller must be reduced and vice versa. Figure 11 represents the
 370 effects of each level of impedance for the same values of reference trajectory in hip
 371 joint (red line) and force (blue line) measured in opposition and in favour of movement.
 372 When a high level of impedance is applied, the real trajectory of the exoskeleton (green
 373 line) follows in a better way the imposed reference (red line). This situation is closer to
 374 trajectory tracking control. The opposite situation occurs with a low level of impedance,
 375 since in this case, the patient is who has more participation in the control of CPWalker,
 376 without becoming a total management of the device.



377

378 **Figure 11. Different levels of impedance control strategy depending on the assistance provided in the hip joint:**
 379 **high impedance, medium impedance and low impedance. Similar values of references (red lines) and forces**
 380 **(blue lines) cause diverse real trajectories (green lines) according to the type of impedance level.**

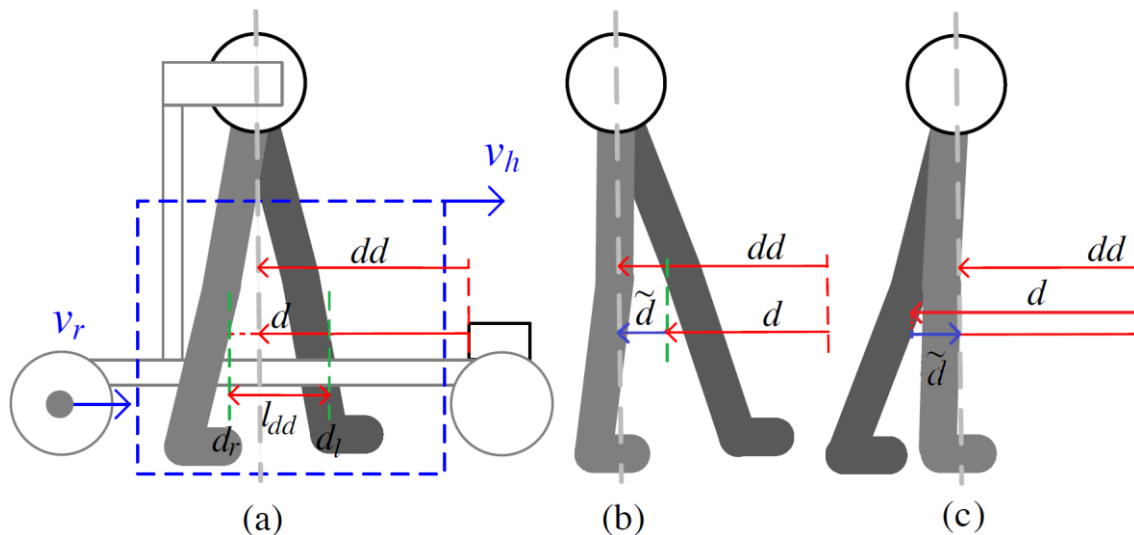
381 Each exoskeleton joint has its own controller with specific parameters estimated
 382 individually for each case and control mode, so the assistance may be generated
 383 separately for each part of the exoskeleton. That means that the type of control may be
 384 selected separately for each joint, but the tracking is ensured in all the exoskeleton
 385 because the reference is sent for all the controllers in each cycle. This possibility
 386 increases the modularity of the system.

387

388 **4.3. Locomotion strategy based on LRF sensor**

389 Working in parallel with a pure patient in charge mode, CPWalker uses a motion
390 control based on the detection of users' legs position (using LRF) and the motors
391 movements (using encoders). The locomotion model is based on the human-walker
392 interaction model presented in [37] and aims at controlling the linear velocity (v_r) of the
393 CPWalker platform, see Figure 12. Following the recommendations of our clinical
394 members, this strategy only enables the control of the velocity of the platform for
395 forward direction.

396 We defined the mean value of the distance of legs measured by the LRF sensor (d) as
397 the variable to be controlled. The control objective is to achieve a desired distance, ($d =$
398 dd), which is identified by the system when the user is placed on the platform. As a
399 result, $\tilde{d} = dd - d$ is defined as the control error, which represents legs motion at three
400 stages depending on its sign: i) when \tilde{d} is close to zero, it represents a stable legs
401 position (double support, Figure 12.a); ii) when \tilde{d} is negative, it represents legs motion
402 in order to perform a step (forward direction, Figure 12.b); and iii) a positive value for \tilde{d}
403 indicates that the legs are behind the trunk axis (Figure 12.c). In order to warranty the
404 patient's safety, this stage stops the platform to restrict only forward motion according
405 to clinician's recommendation.



406

407 **Figure 12. Locomotion model based on LRF of CPWalker: (a) Bilateral foot contact on the floor (double**
 408 **support); (b) Swing phase for left leg and stance phase for right leg; (c) In this condition both legs are behind**
 409 **the platform, which stops the movement**

410 A useful variable for the development of natural human-robot locomotion is human
 411 velocity v_h . The goal is that the velocity of the robotic platform (v_r) follows v_h to
 412 promote user's reliance during therapy. The direct kinematic of Figure 12.a is described
 413 by the Equation 3.

$$\dot{\tilde{d}} = -v_h + v_r \quad (3)$$

414 The inverse kinematic controller obtained from the kinematic model presented in
 415 Equation 3 is shown in Equation 4.

$$v_r = v_h - k \cdot \tilde{d} \quad (4)$$

416 Human gait consists of slow movements, especially in human-robot interaction
 417 scenarios. According to this kinematic approach, using the proposed control law and
 418 assuming a perfect velocity tracking, the control error \tilde{d} converges to zero. This
 419 conclusion becomes after substituting Equation 3 in Equation 4, thus obtaining Equation
 420 5.

$$\dot{\tilde{d}} = \frac{\partial \tilde{d}}{\partial t} = -k \cdot \tilde{d} \quad (5)$$

421 Finally, the control system is exponentially asymptotically stable, as it can be seen in
422 Equation 6.

$$\tilde{d} = \tilde{d}(0) \cdot e^{-kt} \quad (6)$$

423 Figure 12 also shows the l_{dd} signal that represents the distance between both legs
424 produced by the difference between d_l and d_r (defined in Section 3.3). Such signal has a
425 sinusoidal evolution during walking, and it is useful to estimate human velocity (v_h),
426 [37]. v_h is obtained through the product of gait cadence estimation (l_{dd} frequency) and
427 the estimation of step length (l_{dd} amplitude estimation). This estimation is used as a
428 control input of the inverse kinematics controller previously defined.

429 **5. Control Architecture**

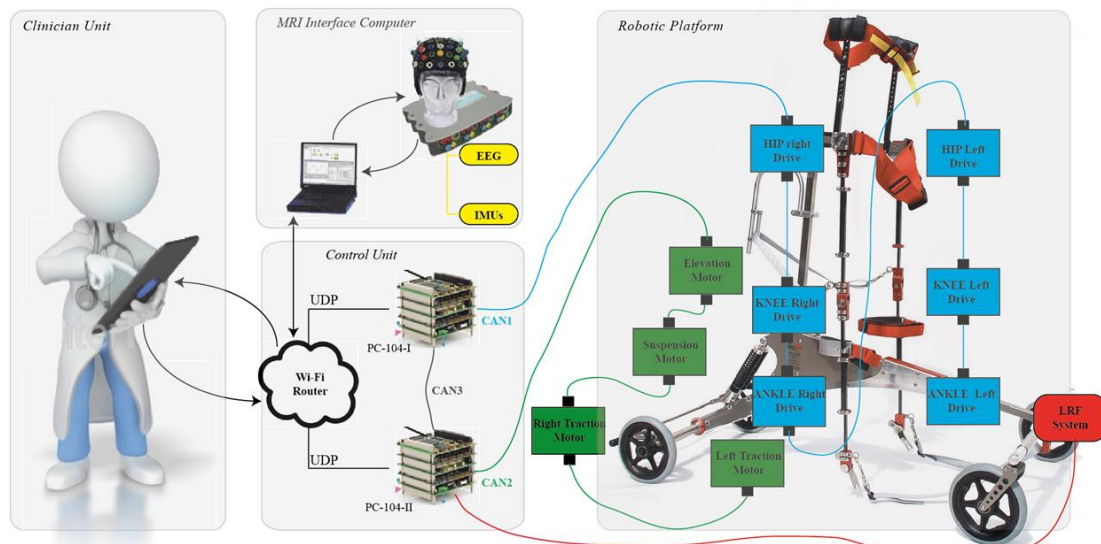
430 The control architecture of CPWalker is shown in Figure 13. It intends to favor the
431 interaction of the whole platform. The control architecture is composed by four main
432 parts:

- 433 1) *Robotic platform* constituted by the exoskeleton and the smart walker with their
434 structure, sensors and actuators, as described in Section 2.
- 435 2) *Control unit*, which receives information from the different sensors of the robotic
436 platform. At the same time, it executes the algorithms for the implementation of the
437 therapies in real time, and generates the control signals for the actuators. The control
438 unit is composed by two PC-104, one responsible for the control of the smart walker,
439 and the other responsible for the exoskeleton. The control of the entire robotic platform
440 is implemented into the MatLab RT environment. This environment enables the

441 development of mathematically complex control strategies in real time. The interface
442 between the MatLab environment and the CPWalker platform is based on a data
443 acquisition boards and on particular drivers developed for the control of motors that
444 communicate through a CAN (Controller Area Network) bus [30].

445 3) *MHRI Remote computer* runs the interaction of MHRI with the user. This computer is
446 able to acquire the information from the different sensors of the multimodal interface
447 (EEG, IMUs, LRF), process it and send the processed information to the control unit for
448 its implementation. This computer also allows the extraction of user parameters during
449 the therapy: identification of EEG patterns, locomotion pattern and interaction force
450 between the user and the device. It is also possible to save all the information retrieved
451 by the sensors for future offline analysis.

452 4) *Clinician unit*, which consists of a smartphone/tablet *device*, that executes an
453 application developed for the interface between the system and the doctor who is using
454 it. This clinical interface, monitors signals and tunes controller parameters in real time
455 during the control strategy execution. It has the following main objectives: i)
456 monitoring and validation of algorithms for CP rehabilitation; ii) data analysis
457 (statistics, algorithms performance, etc.); iii) storage of user information such as clinical
458 and anthropometrics data; and iv) comparison between different robot-based
459 rehabilitation therapies.



460

461 **Figure 13. CPWalker overall control architecture. All sensors in both exoskeleton legs communicate to PC-104-I through a**
 462 **CAN (deterministic real-time) network (CAN1). Motor drivers of the exoskeleton are connected to D/A boards of the PC-**
 463 **104. PC-104-I communicates with PC-104-II via another CAN network (CAN3). PC-104-II is responsible for the control of**
 464 **the traction and PBWS systems. Drivers for controlling the motors of these systems and for reading their sensors**
 465 **communicate with PC-104 via another bus CAN (CAN2).PC-104I and PC104-II together constitutes the control unit of**
 466 **CPWalker platform. Both PC-104 systems are connected to a Wi-Fi hub that enables the communication of both controllers**
 467 **with two external computers: 1) responsible for the acquisition and processing of the MHRI sensors, and 2) a**
 468 **smartphone/tablet that executes the clinician interface and allows clinicians to access platforms information and to control**
 469 **it.**

470 The communication among the different components of the control architecture is
 471 illustrated in Figure 13 and was based on the control architecture defined in [30]. The
 472 communication protocol is based on CAN, a bus topology for the transmission of
 473 messages designed to reduce the volume, complexity and difficulty of wiring and to
 474 achieve a high control speed in real time. To read the message, each driver has an
 475 identifier associated to it, which allows that it can be distinguished from other by the
 476 main controller [38].

477 The communication cycles of the difference being controlled in our system occur at a
 478 fixed rate (1 kHz) set by the control scheme on the control unit. As a result, this
 479 protocol allows for deterministic control and it provides built-in network error detection

480 as, for every message received, each system has to return data information to the control
481 unit. Moreover, the control unit has a robust means to determine the integrity of the
482 network and the correct operation of the joint's actuators. If some failure occurs on the
483 network that cannot be corrected automatically (for instance, a cable disconnection), the
484 control unit instantly shuts down the robotic platform power and stops the CPWalker
485 platform for safety reasons.

486 **6. Technical validation of the different systems**

487 This section describes the technical validation of essential parts of CPWalker platform.
488 It is not a clinical validation, instead it is designed to demonstrate that the different
489 components are integrated into the control strategy and crucial systems are correctly
490 performed. This technical validation enables the clinical staff to design novel therapies
491 for a future use of our platform as benchmark for the experimentation with patients. The
492 local ethical committee at “*Hospital Universitario Niño Jesús*”, gave approval to the
493 technical experiment, and warranted its accordance with the Declaration of Helsinki. All
494 patients were informed beforehand, and signed a written informed consent to
495 participate. Future work will be focused on a proper clinical and functional validation of
496 the performance of our system as a rehabilitation tool.

497 **6.1. Validation of EEG system**

498 The practical implementation of our MHRI faced a number of scientific and
499 technological challenges [39]. Amongst the major scientific challenges was the online
500 detection of movement intention in patients with CP, which had not been properly
501 investigated before. According to Section 3.1, EEG unit has been introduced in the

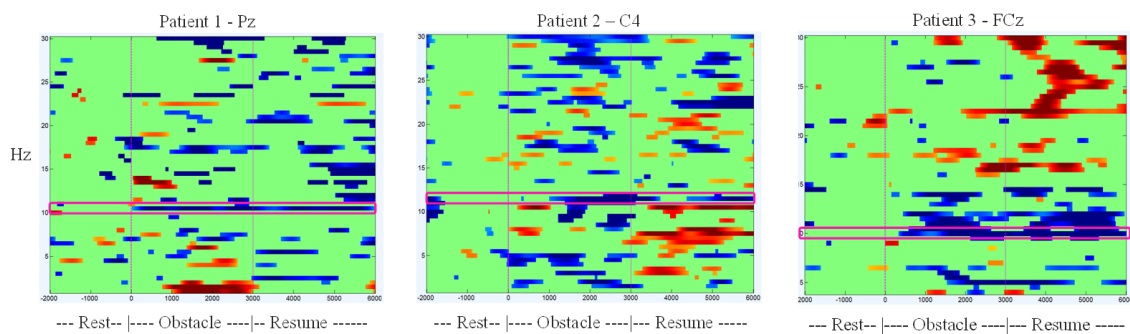
502 rehabilitation through CPWalker platform with the aim of integrating not only the PNS
503 but also the CNS into the rehabilitation therapies of children with CP.

504 A preliminary technical evaluation of the EEG system was done at Niño Jesús Hospital
505 with three children with CP, aged 11, 13 and 15 years respectively. All patients
506 presented no cognitive deficit and they started the first EEG session few days after
507 surgery. Considering that they were weak, we evaluated only the first phase presented in
508 Section 3.1 (patient lying using EEG in combination with virtual reality), with the aim
509 of training them for the future exercises with CPWalker platform.

510 EEG signal was captured from 32 Ag/AgCl electrodes (actiCAP, Brain Products
511 GmbH, Germany), placed over the somatosensory and motor areas, according to the
512 international 10-20 system, while an experimental environment is shown by virtual
513 glasses (Oculus Rift) to each child in a first-person view. The signal was amplified and
514 sampled at 256 Hz. The power values were estimated in overlapping segments of 1.5 s
515 and frequencies between 2-30 Hz in steps of 1 Hz. Welch's method was used to this end
516 (Hamming windows of 1s, 50 % overlapping [40]). The glasses cover the total of the
517 human vision range, so providing an absolutely immersive feeling and, therefore, a
518 realistic visual feedback. The virtual environment consisted of a fantasy world designed
519 with Unreal Development Kit (UDK), an open-source 3D graphic and game engine. It is
520 projected in stereoscopic mode to the glasses for a more realistic experience. Each
521 session corresponds to a walk (in first person) through a defined path around the world.
522 Along the path, there are different 22 obstacles (gates, stones, trees...). Each time the
523 patients got close to an obstacle, the walk stopped and they were instructed to relax for
524 3s, following a phase of walking imagination for other 3s. Then the obstacle disappears
525 and the walk slowly resumes.

526 From these sessions, we selected the pair (channel, frequency band) with the most
 527 pronounced and longest decay of the EEG signals power or PSD (Power Spectral
 528 Density) during the “obstacle disappearing” and “start walking” periods, with respect to
 529 the resting periods. In the BCI-controlled sessions, an obstacle does not disappear until
 530 the selected pair (channel, frequency band) reaches and keeps the learned power
 531 associated to rest for 1s. Analogously, once the obstacle disappears, the walk is not re-
 532 started until the power value reaches the learned desynchronization for 1s. Each session
 533 was performed after two weeks from the last one.

534 Preliminary results indicate that all patients were able to overcome all obstacles and
 535 complete the paths after two sessions. The average time/frequency graphs of the best
 536 channel for each patient are shown in Figure 14 ($p < .05$, with respect to “rest” period;
 537 blue: lower PSD; red: higher PSD). These results demonstrate the ability of the EEG
 538 system to control the start of the rehabilitation strategy, allowing the implementation of
 539 the "Top-Down" approach proposed for this platform.



540

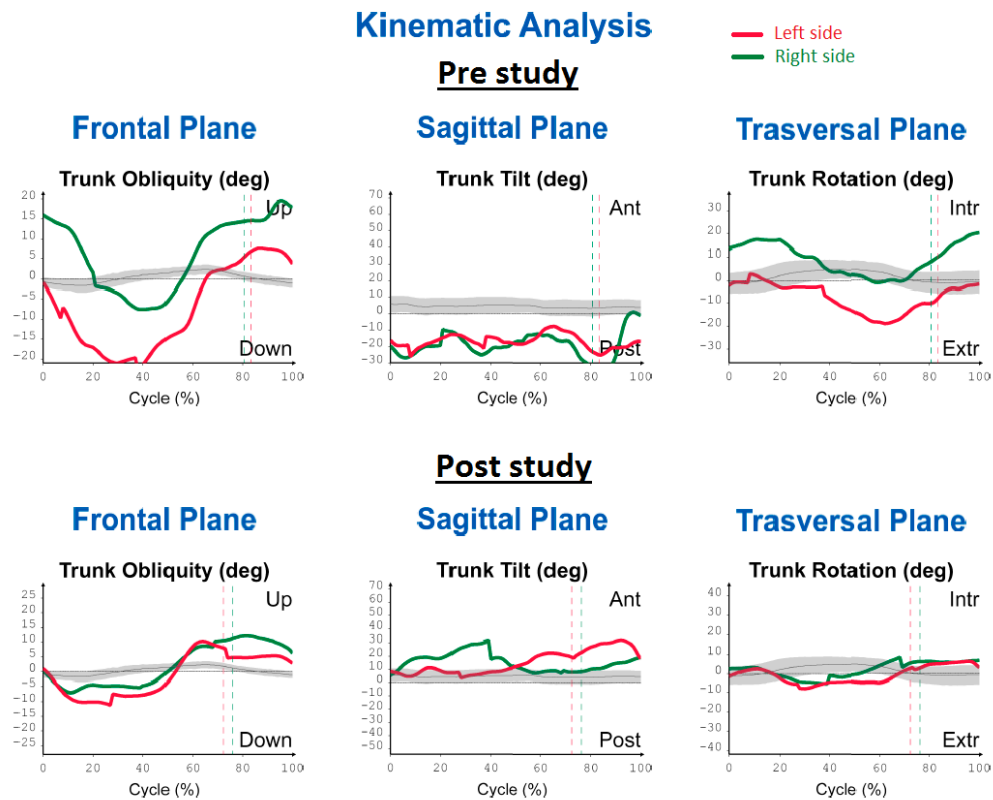
541 **Figure 14.** Average time-frequency graphs showing the most desynchronized pair channel/frequency-bin (pink
 542 box) during automatic sessions for the three patients with CP ($p < .05$, with respect to "rest" period; blue:
 543 lower PSD; red: higher PSD)

544 6.2. Postural control with IMUs based interface

545 Children with CP presented an altered gait pattern with an increased ROM of the trunk
546 during gait. This problem must be addressed as an independent movement limitation
547 and rehabilitation strategies must be oriented to correct it [41]. In order to address this
548 issue we developed a specific posture control therapy based on the CPWalker, that
549 provides feedback to the patients while allow they to move their legs. The rationale of
550 this IMUs based interface is to enhance the cognitive interaction between the child and
551 the robot.

552 Such this therapy was preliminarily evaluated in one child with spastic diplegia in order
553 to assess the usability of the system as a rehabilitation tool in clinical practice. The main
554 objective of this trial was oriented to assess the motor control improvements of the
555 trunk during gait. One IMU sensor was placed on the patient's head and the other on the
556 patient's chest. The exercises consisted on giving acoustic feedback to the user through
557 a disturbing sound when the subject's trunk or head were not in a proper position. At
558 the same time, the patient was walking with CPWalker following the position control
559 strategy.

560 In order to measure the progress of the subject after this robot-based therapy, trunk
561 kinematic data was obtained from 3D gait analysis before and after the experiment. The
562 data collection was performed using an eight infrared cameras system (BTS
563 BioEngineering). Reflective markers were applied on the shoulder girdle (spinous
564 process of C7 and both acromio-clavicular joints). Marker trajectories were processed
565 and analyzed. For comparisons a pre-post graph was performed for this child (Figure
566 15).

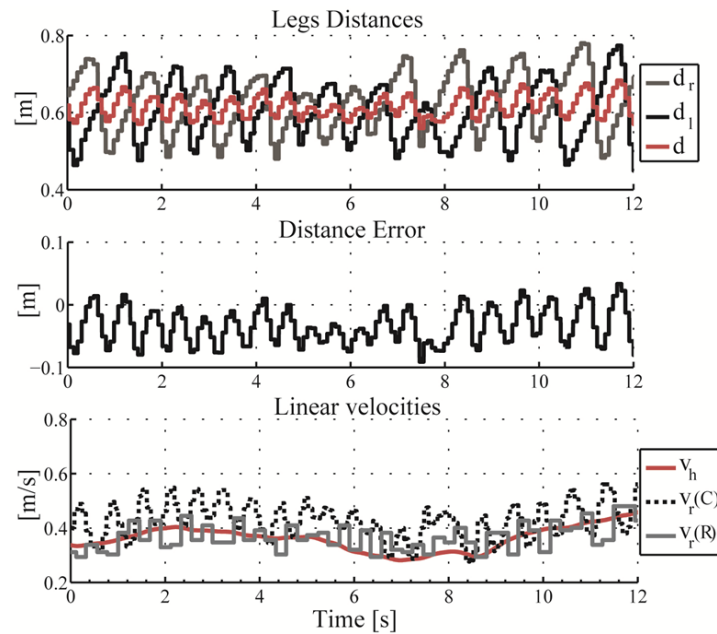


567

568 **Figure 15. Trunk kinematics of the child during the pilot trial. Normal trunk kinematics data is represented in**
 569 **grey. Pre-intervention data is represented above. Post- intervention data is represented below. Left side in red**
 570 **and Right side in green.**

571 **6.3. Validation of locomotion strategy based on LRF sensor**

572 As a representative case, Figure 16 shows the control data recorded during an
 573 experiment for 12 seconds; it corresponds to a patient with CP using the assistance of
 574 CPWalker locomotion controller performing a straight path. Figure 16.a shows the
 575 distance of the legs obtained by the LRF data. \tilde{d} is negative most of the time showing
 576 that the patient is walking in forward direction as can be seen in Figure 16.b. In Figure
 577 16.c the control action $v_r(C)$, which is the CPWalker velocity command, follows (v_h) , as
 578 expected. Finally, there is no significant delay between the control action, $v_r(C)$, and the
 579 CPWalker velocity measured $v_r(R)$ from the encoders of the wheels.



580

581 **Figure 16. Experiment of a CP patient using CPWalker with human velocity changes: (a) Legs position**
 582 **detection from the LRF; (b) Distance error that represents the forward walking; (c) Human velocity**
 583 **estimation (red line), CPWalker velocity commands (segmented line) and CPWalker velocity measured (grey**
 584 **line).**

585 In Figure 16.a, it is possible to observe that the user decreased the step length from the
 586 2th to the 6th second, and it was also increased from the 8th to the 12th seconds. These
 587 changes are reflected in the human velocity estimation (v_h) (see Figure 16.c).
 588 Consequently, both $v_r(C)$ and $v_r(R)$ are updated accordingly and the platform is able to
 589 follow the user (see Figure 16.c).

590 Although v_h has the majority of the contribution in the control action (see Figure 16.c),
 591 there is also an oscillatory component. Such component is the contribution of \tilde{d} to the
 592 adjustment of the CPWalker motion during each step. Considering that the trunk is
 593 fixed to the platform, when the user performs a step (swing phase), \tilde{d} assumes a
 594 negative value. Consequently, the control action is incremented to move the CPWalker
 595 with the human trunk in order to achieve a zero error. Therefore, the velocity of
 596 CPWalker is also proportionally incremented with each step (swing phase) and it is

597 reduced when the step is finished (double support). This strategy showed a natural
598 Human-CPWalker interaction during preliminary experiments.

599 **7. Discussion and Conclusions**

600 This paper has presented a novel robotic system for gait rehabilitation in children with
601 CP and similar motor disorders, which was developed in the framework of the project
602 CPWalker. The overall aim of this project is to develop a robotic platform to provide
603 means for testing new therapies for gait rehabilitation in subjects with CP. This paper
604 has been focused on the conceptualization, development and technical validation of this
605 robotic platform.

606 The robotic trainer integrates a robotic exoskeleton, a neuroprosthesis, and a smart
607 walker. The combination of these devices into the integrated platform enables the
608 therapists to implement novel interventions for gait training in CP. CPWalker is the first
609 trainer with dynamic bodyweight support and active driven gait in real environments.

610 CPWalker is equipped with kinematic and kinetic sensors. In addition, the interaction of
611 the user with the platform is implemented through a MHRI based on EEG, IMUs and
612 LRF sensors. These sensors will be also used to both provide a real-time biofeedback to
613 the children, and an off-line report to therapists and caregivers on therapy progress and
614 patient's motor evolution. Feedback information will be derived from the MHRI system,
615 e.g. trends in involuntary movements like effort during motor planning; and from robot
616 information, e.g. trajectories and driving time. The software tool developed to interface
617 the clinician with the robotic platform will allow the therapist to configure the
618 intervention and to obtain feedback of its outcome, both during the rehabilitation
619 session and offline, in order to evaluate the patient's evolution.

620 Results demonstrated that the different systems of the robotic platform are integrated
621 and performing. Preliminary results show the capacity of the novel robotic platform to
622 serve as a rehabilitation tool [8]. This platform will allow authors to precisely evaluate
623 the effects of different robot-based control strategies on population with CP. The
624 obtained outcomes with future clinical validations aim at providing important results to
625 understand and justify the use of robotic therapy.

626 This project is built on vast previous clinical evidence that neural plasticity is the central
627 core of motor development, and on studies suggesting that robot-mediated intensive
628 therapy is beneficial for improving functional recovery [42]. Nevertheless, current level
629 of evidence regarding the efficacy of new technologies in the rehabilitation process still
630 remains scarce. These approaches need to be refined and critically analyzed to
631 determine their functional benefit for children with different levels of sensory-motor,
632 cognitive impairment or both.

633 The presented platform enables the development of different therapies based on the
634 "Top-Down" approach. Future studies using the robotic platform are in place and
635 involve follow-up measurement to determine if gains will have long-term and lasting
636 impact for children with CP.

637 **Acknowledgements**

638 The work presented in this paper has been carried out with the financial support from
639 the Ministerio de Economía y Competitividad of Spain, under Contract DPI2012-
640 39133-C03-01.

641 Authors would like to thank *Made for Movement* company for providing and supporting
642 us in the mechanical design of a NF-Walker device. Authors also would like to thank
643 the following Brazilian agencies for supporting this research: CNPq (Processes

644 308529/2013-8), CAPES/Brazil (Process 8887.095626/2015-01) and FAPES/Brazil
645 (Process 67566480).

646 We greatly appreciate the efforts and contributions from all the testing subjects and their
647 families.

648

649 **References**

- 650 [1] M. Bax, D. M. Frcp, P. Rosenbaum, B. Dan, H. Universitaire, R. Fabiola, U. L.
651 De Bruxelles, M. Goldstein, and D. D. Pt, “Review Proposed definition and
652 classification of cerebral palsy , April 2005 Executive Committee for the
653 Definition of Cerebral Palsy,” *Dev. Med. Child Neurol.*, no. April, pp. 571–576,
654 2005.
- 655 [2] A. Johnson, “Prevalence and characteristics of children with cerebral palsy in
656 Europe.,” *Dev. Med. Child Neurol.*, vol. 44, no. 9, pp. 633–40, Sep. 2002.
- 657 [3] S. Winter, A. Autry, C. Boyle, and M. Yeargin-Allsopp, “Trends in the
658 prevalence of cerebral palsy in a population-based study.,” *Pediatrics*, vol. 110,
659 no. 6, pp. 1220–5, Dec. 2002.
- 660 [4] D. L. Damiano, K. E. Alter, and H. Chambers, “New clinical and research trends
661 in lower extremity management for ambulatory children with cerebral palsy.,”
662 *Phys. Med. Rehabil. Clin. N. Am.*, vol. 20, no. 3, pp. 469–91, Aug. 2009.
- 663 [5] P. W. Duncan, K. J. Sullivan, A. L. Behrman, S. P. Azen, S. S. Wu, S. E.
664 Nadeau, B. H. Dobkin, D. K. Rose, J. K. Tilson, S. Cen, and S. K. Hayden,
665 “Body-weight-supported treadmill rehabilitation after stroke.,” *N. Engl. J. Med.*,
666 vol. 364, no. 21, pp. 2026–36, May 2011.
- 667 [6] S. E. Fasoli, B. Ladenheim, J. Mast, and H. I. Krebs, “New horizons for robot-
668 assisted therapy in pediatrics.,” *Am. J. Phys. Med. Rehabil.*, vol. 91, no. 11 Suppl
669 3, pp. S280-9, Nov. 2012.
- 670 [7] A. Calanca, S. Piazza, and P. Fiorini, “A motor learning oriented, compliant and
671 mobile Gait Orthosis,” *Appl. Bionics Biomech.*, vol. 9, no. 1, pp. 15–37, 2012.

- 672 [8] C. Bayón, S. Lerma, O. Ramírez, J. I. Serrano, M. D. Del Castillo, R. Raya, J. M.
673 Belda-Lois, I. Martínez, and E. Rocon, “Locomotor training through a novel
674 robotic platform for gait rehabilitation in pediatric population: short report,” *J.*
675 *Neuroeng. Rehabil.*, vol. 13, no. 1, p. 98, 2016.
- 676 [9] I. Borggraefe, M. Klaiber, T. Schuler, B. Warken, S. A. Schroeder, F. Heinen,
677 and A. Meyer-Heim, “Safety of robotic-assisted treadmill therapy in children and
678 adolescents with gait impairment: a bi-centre survey.,” *Dev. Neurorehabil.*, vol.
679 13, no. 2, pp. 114–9, Jan. 2010.
- 680 [10] J.-M. Belda-Lois, S. Mena-del Horno, I. Bermejo-Bosch, J. C. Moreno, J. L.
681 Pons, D. Farina, M. Iosa, M. Molinari, F. Tamburella, A. Ramos, A. Caria, T.
682 Solis-Escalante, C. Brunner, and M. Rea, “Rehabilitation of gait after stroke: a
683 review towards a top-down approach.,” *J. Neuroeng. Rehabil.*, vol. 8, no. 1, p.
684 66, Jan. 2011.
- 685 [11] A. C. Lo, P. D. Guarino, L. G. Richards, J. K. Haselkorn, G. F. Wittenberg, D. G.
686 Federman, R. J. Ringer, T. H. Wagner, H. I. Krebs, B. T. Volpe, C. T. Bever, D.
687 M. Bravata, P. W. Duncan, B. H. Corn, A. D. Maffucci, S. E. Nadeau, S. S.
688 Conroy, J. M. Powell, G. D. Huang, and P. Peduzzi, “Robot-assisted therapy for
689 long-term upper-limb impairment after stroke.,” *N. Engl. J. Med.*, vol. 362, no.
690 19, pp. 1772–83, May 2010.
- 691 [12] S. Wang, L. Wang, C. Meijneke, E. Van Asseldonk, T. Hoellinger, G. Cheron, Y.
692 Ivanenko, V. La Scaleia, F. Sylos-labini, M. Molinari, F. Tamburella, F.
693 Thorsteinsson, M. Ilzkovitz, J. Gancet, Y. Nevatia, R. Hauffe, and H. Van Der
694 Kooij, “Design and Evaluation of the Mindwalker Exoskeleton,” vol. 23, no. 2,
695 pp. 277–286, 2015.

- 696 [13] A. Meyer-Heim and H. J. a van Hedel, “Robot-assisted and computer-enhanced
697 therapies for children with cerebral palsy: current state and clinical
698 implementation.,” *Semin. Pediatr. Neurol.*, vol. 20, no. 2, pp. 139–45, Jun. 2013.
- 699 [14] N. Smania, M. Gandolfi, V. Marconi, A. Calanca, C. Geroin, S. Piazza, P.
700 Bonetti, P. Fiorini, A. Consentino, C. Capelli, D. Conte, M. Bendinelli, D.
701 Munari, P. Ianes, A. Fiaschi, and A. Picelli, “Applicability of a new robotic
702 walking aid in a patient with cerebral palsy,” *Euro J Phys Rehabil Med*, vol. 47,
703 no. 0, pp. 1–7, 2011.
- 704 [15] S. C. Cramer, M. Sur, B. H. Dobkin, C. O’Brien, T. D. Sanger, J. Q.
705 Trojanowski, J. M. Rumsey, R. Hicks, J. Cameron, D. Chen, W. G. Chen, L. G.
706 Cohen, C. Decharms, C. J. Duffy, G. F. Eden, E. E. Fetz, R. Filart, M. Freund, S.
707 J. Grant, S. Haber, P. W. Kalivas, B. Kolb, A. F. Kramer, M. Lynch, H. S.
708 Mayberg, P. S. McQuillen, R. Nitkin, A. Pascual-Leone, P. Reuter-Lorenz, N.
709 Schiff, A. Sharma, L. Shekim, M. Stryker, E. V. Sullivan, and S. Vinogradov,
710 “Harnessing neuroplasticity for clinical applications,” *Brain*, vol. 134, no. 6, pp.
711 1591–1609, 2011.
- 712 [16] H. van der Kooij, B. Koopman, and E. H. F. van Asseldonk, “Body weight
713 support by virtual model control of an impedance controlled exoskeleton
714 (LOPES) for gait training.,” *Conf. Proc. IEEE Eng. Med. Biol. Soc.*, vol. 2008,
715 pp. 1969–1972, 2008.
- 716 [17] R. Palisano, P. Rosenbaum, S. Walter, D. Russell, E. Wood, and B. Galuppi,
717 “Gross Motor Function Classification System,” *Dev. Med. Child Neurol.*, vol. 39,
718 pp. 214–223, 1997.
- 719 [18] K. Willoughby, K. Dodd, and N. Shields, “A systematic review of the

- 720 effectiveness of treadmill training for children with cerebral palsy,” *Disabil.*
721 *Rehabil.*, 2009.
- 722 [19] H. Barbeau and M. Visintin, “Optimal outcomes obtained with body-weight
723 support combined with treadmill training in stroke subjects,” *Arch. Phys. Med.*
724 *Rehabil.*, vol. 84, pp. 1458–65, 2003.
- 725 [20] A. Cullell, J. C. Moreno, E. Rocon, A. Forner-Cordero, and J. L. Pons,
726 “Biologically based design of an actuator system for a knee-ankle-foot orthosis,”
727 *Mech. Mach.Theory*, vol. 44, no. 4, pp. 860–872, 2009.
- 728 [21] E. Rocon, J. M. Belda-Lois, A. F. Ruiz, M. Manto, J. C. Moreno, and J. L. Pons,
729 “Design and validation of a rehabilitation robotic exoskeleton for tremor
730 assessment and suppression,” *IEEE Trans. neural Syst. Rehabil. Eng.*, vol. 15,
731 no. 3, pp. 367–378, Sep. 2007.
- 732 [22] G. Colombo, M. Joerg, R. Schreier, and V. Dietz, “Treadmill training of
733 paraplegic patients using a robotic orthosis.,” *J. Rehabil. Res. Dev.*, vol. 37, no. 6,
734 pp. 693–700, 2000.
- 735 [23] J. Doke, J. M. Donelan, and A. D. Kuo, “Mechanics and energetics of swinging
736 the human leg.,” *J. Exp. Biol.*, vol. 208, no. Pt 3, pp. 439–445, 2005.
- 737 [24] M. T. Robert, R. Guberek, H. Sveistrup, and M. F. Levin, “Motor learning in
738 children with hemiplegic cerebral palsy and the role of sensation in short-term
739 motor training of goal-directed reaching,” *Dev. Med. Child Neurol.*, vol. 55, no.
740 12, pp. 1121–1128, 2013.
- 741 [25] E. Abd El-Kafy and H. El-Basatini, “Effect of postural balance training on gait
742 parameters in children with cerebral palsy.,” *Am. J. Phys. Med. Rehabil.*, vol. 93,
743 no. 11, pp. 938–947, 2014.

- 744 [26] R. Dewar, S. Love, and L. M. Johnston, “Exercise interventions improve postural
745 control in children with cerebral palsy: a systematic review.” *Dev. Med. Child*
746 *Neurol.*, Dec. 2014.
- 747 [27] N. Bellotto and Huosheng Hu, “Multisensor-Based Human Detection and
748 Tracking for Mobile Service Robots,” *IEEE Trans. Syst. Man, Cybern. Part B*,
749 vol. 39, no. 1, pp. 167–181, Feb. 2009.
- 750 [28] T. Pallejà, M. Teixidó, M. Tresanchez, and J. Palacín, “Measuring gait using a
751 ground laser range sensor,” *Sensors*, vol. 9, no. 11, pp. 9133–9146, 2009.
- 752 [29] S. Hussain, S. Q. Xie, and G. Liu, “Robot assisted treadmill training:
753 Mechanisms and training strategies,” *Med. Eng. Phys.*, vol. 33, no. 5, pp. 527–
754 533, 2011.
- 755 [30] M. Bortole, A. Venkatakrishnan, F. Zhu, J. C. Moreno, G. E. Francisco, J. L.
756 Pons, and J. L. Contreras-Vidal, “The H2 robotic exoskeleton for gait
757 rehabilitation after stroke: early findings from a clinical study,” *J. Neuroeng.*
758 *Rehabil.*, vol. 12, no. 1, p. 54, 2015.
- 759 [31] S. Jezernik, G. Colombo, and M. Morari, “Automatic Gait-Pattern Adaptation
760 Algorithms for Rehabilitation With a 4-DOF Robotic Orthosis,” *IEEE Trans.*
761 *Robot. Autom.*, vol. 20, no. 3, pp. 574–582, 2004.
- 762 [32] B. Koopman, E. H. F. van Asseldonk, and H. Van der Kooij, “Speed-dependent
763 reference joint trajectory generation for robotic gait support,” *J. Biomech.*, vol.
764 47, no. 6, pp. 1447–1458, 2014.
- 765 [33] M. Pohl, C. Werner, M. Holzgraefe, G. Kroczyk, J. Mehrholz, I. Wingendorf, G.
766 Hoolig, R. Koch, and S. Hesse, “Repetitive Locomotor Training and
767 physiotherapy improve walking and basic activities of daily living after stroke: a

768 single-blind, randomized multicentre trial,” *Clin. Rehabil.*, vol. 21, pp. 17–27,
769 2007.

770 [34] B. Husemann, F. Muller, C. Krewer, S. Heller, and E. Koenig, “Effects of
771 locomotion training with assistance of a robot-driven gait orthosis in hemiparetic
772 patients after stroke: A randomized controlled pilot study,” *Stroke*, vol. 38, pp.
773 349–354, 7AD.

774 [35] N. Hogan, “Impedance Control: An Approach to Manipulation: parts I, II and
775 III,” *J. Dyn. Syst. Meas. Control*, vol. 107, 1985.

776 [36] R. Riener, L. Lünenburger, S. Jezernik, M. Anderschiz, G. Colombo, and V.
777 Dietz, “Patient-Cooperative Strategies for Robot-Aided Treadmill Training : First
778 Experimental Results,” *Trans. neural Syst. Rehabil. Eng.*, vol. 13, no. 3, pp. 380–
779 394, 2005.

780 [37] C. A. Cifuentes, C. Rodriguez, A. Frizera-Neto, T. F. Bastos-Filho, and R.
781 Carelli, “Multimodal Human–Robot Interaction for Walker-Assisted Gait,” *IEEE*
782 *Syst. J.*, pp. 1–11, 2014.

783 [38] M. Bortole, “Robotic Exoskeleton with an assist-as-needed control strategy for
784 gait rehabilitation after stroke,” Universidad Carlos III, 2014.

785 [39] E. Rocon, J. A. Gallego, L. Barrios, A. R. Victoria, J. Ibanez, D. Farina, F.
786 Negro, J. L. Dideriksen, S. Conforto, T. D’Alessio, G. Severini, J. M. Belda-
787 Lois, L. Z. Popovic, G. Grimaldi, M. Manto, and J. L. Pons, “Multimodal BCI-
788 mediated FES suppression of pathological tremor.,” *Conf. Proc. Annu. Int. Conf.*
789 *IEEE Eng. Med. Biol. Soc. IEEE Eng. Med. Biol. Soc. Conf.*, vol. 2010, pp.
790 3337–40, Jan. 2010.

791 [40] P. Welch, “The use of fast fourier transform for the estimation of power spectra:

- 792 A method based on time averaging over short, modified periodograms,” *IEEE*
793 *Trans. Audio Electroacoust.*, vol. 15, no. 2, 1967.
- 794 [41] L. Heyrman, H. Feys, G. Molenaers, E. Jaspers, D. Monari, A. Nieuwenhuys, and
795 K. Desloovere, “Altered trunk movements during gait in children with spastic
796 diplegia: Compensatory or underlying trunk control deficit?,” *Res. Dev. Disabil.*,
797 vol. 35, no. 9, pp. 2044–2052, 2014.
- 798 [42] T. Sukal-Moulton, T. Clancy, L.-Q. Zhang, and D. Gaebler-Spira, “Clinical
799 application of a robotic ankle training program for cerebral palsy compared to the
800 research laboratory application: does it translate to practice?,” *Arch. Phys. Med.*
801 *Rehabil.*, vol. 95, no. 8, pp. 1433–40, Aug. 2014.
- 802